

Rare and Rare Earth Elements in Lateritized Bauxites of the Chadobets Uplift (Siberian Platform)

N. M. Boeva^{a,*}, A. D. Slukin^a, E. S. Shipilova^a, M. A. Makarova^a, F. V. Balashov^a, E. A. Zhegallo^b,
L. V. Zaytseva^b, and Academician N. S. Bortnikov^a

Received March 24, 2021; revised May 26, 2021; accepted May 27, 2021

Abstract—The mineral and chemical composition of bauxites from the Chadobets uplift of the Siberian Platform is the total product of laterites on aluminosilicate rocks (source of aluminum) and on alkaline rocks and carbonatites (source of rare earth elements (REEs), Nb, Ta, Th, U, etc.). The laterization of these rocks and subsequent denudation led to the formation of unique bauxite deposits with a high content of rare and REEs. Supergene minerals of the laterite weathering crust are in a dispersed microcrystalline and amorphous state, which complicates their study and the choice of methods for extracting useful components. Precision methods were used to establish the forms and compositions of the main supergene minerals, biomineral films, biomorphoses, and the distribution of rare and rare earth elements in them.

Keywords: bauxite, laterite, gibbsite, rare and rare earth elements

DOI: 10.1134/S1028334X21090038

INTRODUCTION

Laterite weathering crusts (LWCs) are sources of deposits of many minerals: iron, manganese, gold, bauxite, and rare and rare earth elements (REE). Laterites are products of the highest degree of weathering. They are characterized by a complete (or almost complete) loss of silicon, alkaline, and alkaline earth elements and a relative residual accumulation of hydrolysate elements: Al, Fe, Mn, Th, etc., oxides and phosphates. In addition, in the process of laterite formation, the minerals composing them continuously go through the stages of colloid formation and the sorption of chemical elements from solutions seeping downward and from solutions rising during evapotranspiration from the lower WC zones. Thus, they are enriched with the above elements, as well as the contents of Ti, Th, U, Pb, Zn, REE, Y, Ba, Sr, Co, Ni, etc.

Deposits of rare metal WC zones have been well studied [1–4]. REEs and rare elements were used as an indicator to determine the nature of the parent rock and chemical processes changing the profile during weathering, and their relationship with supergene minerals [5–8]. The study of the behavior of REEs in

bauxites of the KMA made it possible to clarify the zoning of the weathering crust and assess the degree of transformations associated with superimposed processes [9]. In chlorite shales in southern Cameroon, REE enrichment at the base of bauxite deposits is explained by an increase in pH around the parent rock, as well as by the presence of mineral ligands during bauxitization [10].

Our goal is to study rare-metal elements and REEs in bauxites of the Chadobets uplift. The bauxites of the Tsentral'noe deposit were formed over quartz–muscovite–feldspar schists penetrated by a complex of alkaline ultrabasic rocks, including the carbonatite bodies of various morphology. Carbonatites of the Chadobets uplift have commercial concentrations of REEs and rare elements [4]. In the process of further lateritization in bauxites, which are not the highest quality aluminum raw materials, uniquely high concentrations of titanium, rare elements and REEs, phosphorus, and strontium were formed, which allows them to be considered as a complex raw material. With the selected processing scheme, deposits of this type can be highly profitable. It seems that the results of a detailed study of the morphology and composition of supergene rare and REE minerals present in bauxite ores will be of practical importance in choosing the most rational methods for processing low-grade bauxite, in preparing a scheme for the associated extraction of useful components (Fe, Ti, Ga, V), including trace elements (REEs, Y, Ba, P, U, Th, Nb, Ta). The construction of the Karabula-Yarki railway and the commissioning of the Boguchanskii aluminum plant built

^a Institute of Geology of Ore Deposits, Petrography, Mineralogy, and Geochemistry, Russian Academy of Sciences, Moscow, 119017 Russia

^b Borissiak Paleontological Institute, Russian Academy of Sciences, Moscow, 117647 Russia

*e-mail: boeva@igem.ru

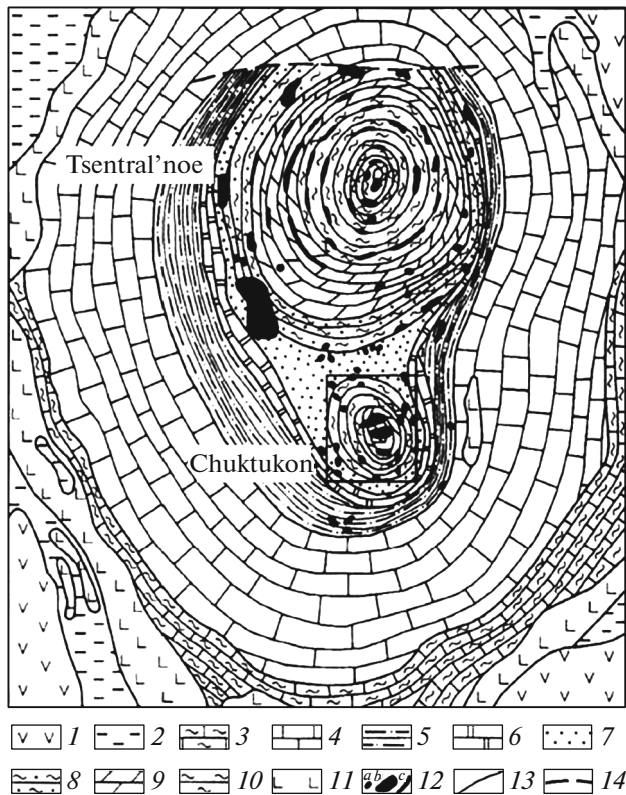


Fig. 1. Scheme of the geological structure of the Chadobets uplift with removed Upper Paleogene and Albian–Eocene deposits: (1) Lower Triassic formations; (2) middle–upper Carboniferous deposits; (3) Middle–Upper Cambrian deposits; (4) Lower Cambrian carbonate rocks; Upper Proterozoic deposits of the formation: (5) Togonskaya; (6) unnamed; (7) Medvekovskaya; (8) Bruskaya; (9) carbonate–terrigenous Terinovskaya, Chuktukonskaya, and Dolchikovskaya formations; (10) Semyonovskaya; (11) traps; (12) alkaline ultrabasic rocks and carbonatites of the Chadobets complex: *a*, explosion pipe; *b*, stock-like bodies; *c*, sills; (13) geological boundaries; (14) tectonic disturbances [1, 4].

120 km away from it and the recently opened Boguchanskaya hydroelectric power station are prerequisites for solving the problem of development and presuppose the start of exploitation of these deposits.

GEOLOGICAL POSITION OF THE CHADOBETS UPLIFT

The Chadobets uplift is in the southwestern part of the Siberian platform between the Angara and Podkamennaya Tunguska rivers. It is a brachyantoclinal structure with axes of 46 and 35 km. It is complicated by two protrusions–cores: the northern one with the Tsentral'noe deposit and the southern one with Chuktukon. They are composed of Precambrian sediments cut through by alkaline ultrabasic rocks in the form of stocks, dikes, sills, kimberlite pipes, and carbonatite bodies [4].

In the Cretaceous, in a tropical hot, variably humid climate, lateritization processes took place on the Siberian platform. Their products have been preserved in the form of numerous, partially eroded LWCs on traps and associated small sedimentary bauxite deposits. There are manifestations of ferromanganese ocher over carbonatites and thick (8.5 m) remnants of gibbsitic bauxite over schists at the Tsentral'noe bauxite deposit WC. The gibbsitic bauxites are identical in their textural and structural features and mineral and chemical composition of the main rock-forming components to lateritic bauxites on similar rocks in India, Australia, and Guinea [11–14]. The Tsentral'noe deposit, composed of pisolitic–detrital bauxite, is in erosional depressions on the surface of the northern dome. The fragments contain pseudomorphic laterites over all the underlying rocks.

Pseudomorphic bauxites of the Tsentral'noe deposit and the presence of gibbsite in lateritized carbonatites of the Terinovskoe and Chuktukonskoe ledges of the Chadobets uplifts are reliable indicators that they are products of a single weathering process.

It was found that lateritic bauxites formed from quartz–muscovite–feldspar schists consist of gibbsite (up to 62 wt % Al_2O_3), boehmite, corundum, goethite, hematite, maghemite, anatase, kaolinite, and quartz. Alkaline ultrabasic laterites contain 3–13 wt % Al_2O_3 and up to 32 wt % TiO_2 in the form of supergene anatase pseudomorphs over octahedral perovskite crystals. Laterites over carbonatites are composed of Fe–Mn–ocher with abundant nests of powder of supergene monazite with a lanthanides content of up to 14.4 wt %. The southern dome is dominated by weathering crusts of carbonatites with monazite, rhabdophanes, drachite, florensit, and secondary, supergene pyrochlores (–Ce, –Y, –Sr, and –Ba). Denudation of these laterites led to the formation of unique deposits of sedimentary bauxite with high contents of REE, Sr, Ba, P, U, Th, and Ti. Limestones of the Upper Cambrian are widespread along the edges of the uplift, where redeposited lateritized dolerites (deposits Punya, Ibdzhibdek, Verkhne-Terinskoe and others) occur in karst depressions. Fragments of laterites consist of gibbsite, in some places with an admixture of nordstrandite. Pisolitic bauxites are composed of gibbsite with admixtures of boehmite, diaspor, corundum, and nordstrandite. At Chuktukon, weathering also reached its highest stage, up to the complete removal of Si, Ca, Mg, Na, and K [1, 11].

METHODS

This study was carried out using scanning (SEM) CamScan 4 (Cambridge) and TESCAN VEGA IIXMU (Tescan) electron microscopes equipped with an energy dispersive spectrometer (EDS). Synchronous thermal analysis (STA) was performed on an STA 449 F1 Jupiter Netzsch device. The measurements

Table 1. Chemical composition (wt %) of bauxite, Tsentral'noe

Component	Bauxites									
	2152	2150	2147	2145	2143	1530	2382	2381	1535	1411
SiO ₂	2.68	3.76	2.05	2.63	1.35	9.55	0.78	1.11	1.86	2.28
TiO ₂	8.1	8.29	8.86	9.58	9.42	10	5.64	3	9.24	7.31
Al ₂ O ₃	49.73	40.18	36.75	43	45.62	38.78	38.36	33.89	31.96	27.19
Fe ₂ O ₃	10.89	7.21	24.94	18.18	13.56	0.86	28.19	40.58	35.26	40.1
FeO	no	no	no	no	no	1.54	no data	no data	3.16	0.22
MnO	no data	no data	no data	no data	no data	no	0.21	0.07	no data	0.32
MgO	0.28	0.44	0.42	0.28	0.29	0.71	0.3	no data	0	0.68
CaO	no	2.94	0.5	0.3	0.42	0.83	0.28	no data	0.34	0.68
Na ₂ O	0.05	0.07	0.05	0.04	0.04	0.06	no data	0.07	0.1	0.2
K ₂ O	0.03	0.05	0.02	0.02	0.02	0.07	no data	no data	0.03	0.06
BaO	no	2.42	0.42	no	no	1.68	no data	no data	no data	no data
SO ₃	no	0.66	0.22	no	no data	0.87	no data	no data	no data	no data
K ₂ O ₃	0.08	0.09	0.13	0.11	0.13	no data	no data	no data	no data	no data
P ₂ O ₅	3.28	15.5	2.39	2.34	2.32	6.96	0.91	0.49	1.17	0.5
TR ₂ O ₃	2.27	1.13	1.13	2.22	2.12	2.05	no data	no data	no data	no data
CO ₂	0.89	0.46	1.16	0.58	no	0.43	no data	no data	no data	no data
LOI	21.45	16.94	20.69	21.33	24.67	21.84	24.11	20.64	17.04	20.22
Sum	100.18	100.14	99.73	100.44	99.96	100.18	98.78	100.25	100.41	99.85

were carried out at a speed of 10°/min in an Ar atmosphere in crucibles with closed lids at a temperature of up to 1050°C. The sample weight was ~40 mg. The chemical composition of bauxite was determined using an Axios PANalytical X-ray fluorescence spectrometer.

RESULTS AND DISCUSSION

According to XRD data (Table 1), the SiO₂ content in bauxite varies from 1.11 to 9.55 wt %. The TiO₂ content varies from 3 to 10 wt %; Al₂O₃, from 27.19 to 49.73 wt %; and Fe₂O₃, from 0.84 to 45.82 wt %. Na₂O and K₂O are in approximately the same ranges from 0.02 to 0.1 wt %, and P₂O₅, from 0.49 to 15.5 wt %.

Nests and layers of various minerals with a high content of REEs and rare metals were revealed in the bauxite. We studied them by means of SEMs, which made it possible to see the crystal morphology of most minerals and substantiate their genesis.

Crandallite CaAl₃[PO₄]₂(OH)₅ · H₂O was found in veins and nests 2 × 3 cm in size at the boundary of lateritized carbonatites and quartz–muscovite–feldspar schists. Undoubtedly, here its genesis is due to the presence of abundant sources of Al from lateritized aluminosilicates composing schists, as well as Ca and P, which are released during the weathering of apatite and carbonates. In addition, crandallite often contains

Ce (up to 0.08 wt %) and is accompanied by other minerals of the same alunite group, in which cations are represented by Ba (gorseixite), Sr (goyazite), and Pb (plumbogummite). Crandallite has the form of white transparent radial-radiating aggregates consisting of thin plates covered with sparkling pyramidal crystals (Fig. 2b). This mineral was identified by means of CTA. The differential scanning calorimetry (DSC) curves show three endothermic effects with maxima at 349, 457.5, and 527.7°C, associated with the dehydroxylation of crandallite. The weight loss is 13.64%. The loss of hydroxyl groups is accompanied by destruction of the mineral structure. The exothermic effect with a maximum temperature of 834.7°C is associated with its recrystallization. The endothermic effect with maxima at 886 and 920.6°C corresponds to the dissociation of carbonate (Fig. 2b).

Pyrochlore (Na, Ca...)₂(Nb, Ti...)₂O₆ [OH, F] occurs in laterites in the form of octahedral crystals up to 90 μm in size, their twins, and intergrowths with other minerals (Fig. 3a). In the polished sections, pyrochlore crystals are hollow and many of them have a zonal structure and are fractured. The cracks in pyrochlore crystals are filled with goethite and other minerals. The chemical composition of primary and secondary pyrochlore varies over a wide range. The maximum content of Nb₂O₅ is observed in the primary pyrochlore at 72.02 wt %, the minimum corresponds

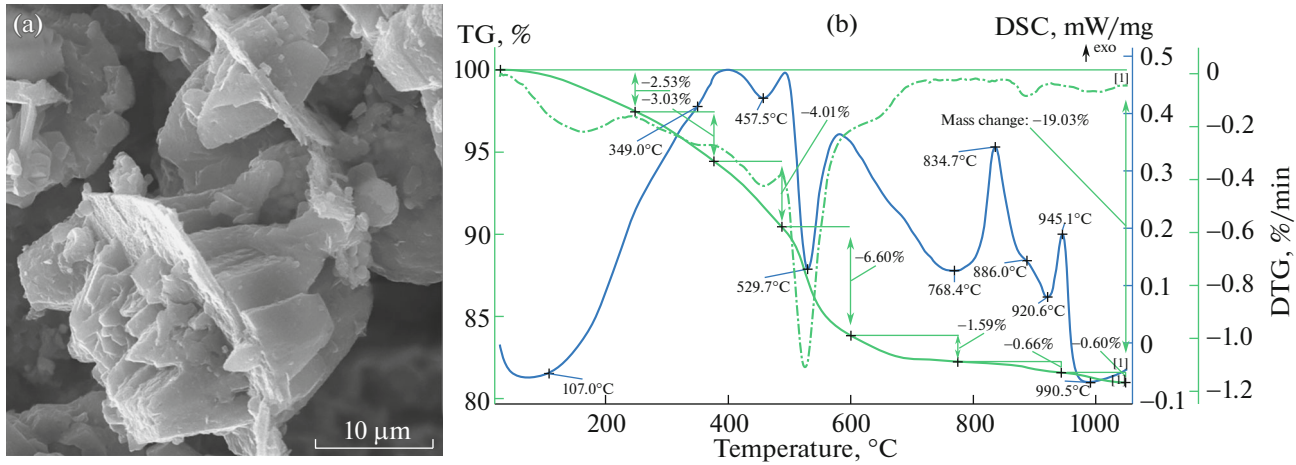


Fig. 2. (a) Crandallite and (b) SEM, curves of thermal analysis.

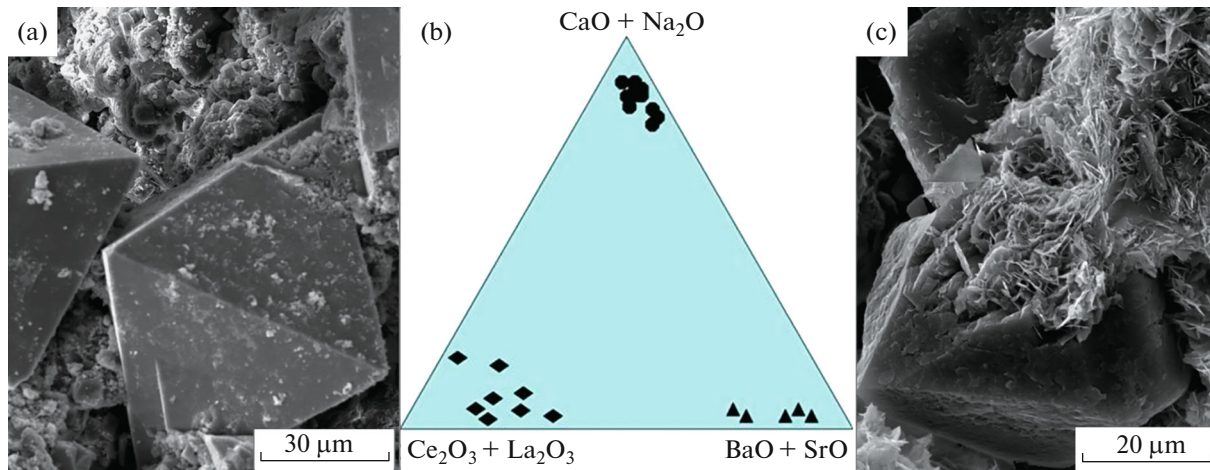


Fig. 3. (a) Primary pyrochlore, (b) composition diagram of pyrochlore, (c) pyrochlore from bauxite. SAM.

to secondary pyrochlore at 58.97 wt %. The TiO_2 content in pyrochlore increases during lateritization. In secondary pyrochlore crystals, CeO_2 varies from 1.86 to 20.13 wt %. La_2O_3 is also found in secondary minerals, from 0.04 to 4.67 wt %. The Cr_2O_3 content in secondary pyrochlore crystals ranges from 0.08 to 0.84 wt %. Fe_2O_3 reaches a maximum of 2.57 wt % and a minimum of 0.12 wt %. The maximum value of CaO is observed in the primary pyrochlore crystals at 20.01 wt %, and the minimum is in the secondary pyrochlores at 0.13 wt %.

During the weathering process, Na and Ca were removed and replaced by Ce, La, Pr, Nd, Y, Ba, and Sr, resulting in the formation of supergene pyrochlore crystals with preferential fixation of light REEs: Ce (pyrochlore-Ce), Sr (pyrochlore-Sr), Ba (pyrochlore-Ba), Y (pyrochlore-Y), the total amount

of which reaches 20–25 wt % (Table 2, Fig. 3b), as well as their varieties of mixed composition, the ratio of which is shown in the three-component diagram (Fig. 3b). Secondary pyrochlore completely retains the appearance of primary crystals but becomes porous and loose (Fig. 3c).

When the mineral is heated, the DSC curve contains one endothermic effect in the temperature range 100–300°C, which is due to mineral dehydration, and two exothermic effects (300–400 and 400–500°C) associated with the transition from the metamict to the crystalline state. Due to the unstable composition of pyrochlore, the maximum temperatures in these intervals vary.

Similar pyrochlore transformations were investigated at the Tomtor deposit [15, 16], where hydrothermal processes are expected to be involved. Without

Table 2. Chemical composition of pyrochlore

Chemical composition (wt %) of pyrochlore crystals								
	63/1	63/2	94/5	17	50	94/3	95/6	95/8
	Primary pyrochlore		Secondary pyrochlore					
Nb ₂ O ₅	69.01	72.02	63.02	69.9	68.71	58.97	68.09	66.13
TiO ₂	7.44	4.62	9.43	0.47	5.44	7.48	4.55	6.77
CeO ₂	no	no	12.35	1.86	5.67	20.13	17.01	15.48
La ₂ O ₃	no	no	0.04	no data	no data	0.61	2.7	4.67
Y ₂ O ₃	0.69	2	0.91	no data	no data	no	1.62	1.85
Cr ₂ O ₃	no	no	0.09	no data	no data	0.84	0.33	0.08
Fe ₂ O ₃	0.44	0.4	0.79	0.12	0.91	2.57	0.65	0.76
CaO	20.01	17.58	2.56	0.13	0.52	4.75	0.45	0.32
MgO	0.02	no	0.39	no data	no data	0.001	0.07	нет
SrO	1.03	1.83	0.81	2.17	13.02	0.07	4.53	3.93
BaO	no	no	9.18	18.24	5.46	4.44	no data	no data
Na ₂ O	1.34	1.15	no	no	no	0.11	no	no
Sum	99.98	99.6	99.57	92.89	99.73	99.98	100	99.99

denying such a possibility at Tomtor, we note that, at Chuktukon and Tsentral'noe, these transformations are the result of exclusively supergene processes under the conditions of the "laterite" climate [17], which is confirmed by the preservation of anchimonomineral pseudomorphic lateritic bauxites over quartz–muscovite–feldspar and other schists.

Biofilms in LWC are formed under conditions of abundant water exchange and mass development of the biome. The biofilm enveloping the gibbsite crystal, which is dominated by Al, contains Fe and Ce impurities (Fig. 4a). As a result of the laterization process, biomineral films are formed, consisting of C, F, P, Ca, Mn, Fe, La, Ce, and Nd (Fig. 4b).

Accumulations of microcrystalline matter with an admixture of spherical bodies 0.5–1.2 μm in size form along the films (Fig. 5). Its composition is dominated by P, Ce, La, and Nd, and the total content of REEs in the rock reaches 14.7 wt %.

Psilomelane (Ba, H₂O)₂Mn₅O₁₀ is found in sedimentary bauxite in the form of scattered ocher grains, incrustations similar to the "black glass head" and their fragments (Fig. 6a). On fresh spalls, their rhythmically banded structure is visible (Fig. 6b). The mineral consists of manganese hydroxide with typical impurities of K, Ca, Zn, and Ba (Fig. 6b). The composition of the layers differs from each other. In some places they alternate with gibbsite. There are local areas enriched with cerium sorbed on the surface. The DSC curve shows three endo-effects with maxima at

120, 620, and 780°C, associated with the sequential removal of hydroxyl groups upon heating. Psilomelane can be used as an indicator when prospecting for REE deposits.

Goethite FeOOH occurs in a variety of forms: from smooth and crumpled biofilms covered with biomorphoses to sheaf-like (Fig. 7a), cruciform, radial-ray, and needle-like crystals (Fig. 7b). The following elements are concentrated in the form of biofilms between goethite crystals along microcracks: Ca, Mn, Zn, Ba, and La. In bauxites, even low-iron ones, gibbsite crystals are dotted with single or numerous idiomorphic lamellar crystals up to 0.8–0.4 μm in size. Goethite is not a rare earth concentrator, but fine ocher mechanically includes any rare earth minerals and the total REE content reaches 10–20 wt %.

Kaolinite Al₄[Si₄O₁₀](OH)₈ in bauxite is sporadically dispersed in the form of separate scales and relics of wormlike intergrowths with imperfect structure (Fig. 8a). The more corroded the surface of the crystals, the more it absorbs chemical elements from the surrounding space (Fig. 8b, inset). Dehydroxylation of kaolinite occurs on the DSC curve in the temperature range 400–600°C with a maximum at 497°C. The asymmetry index is 2.7, which corresponds to a very imperfect structure of the mineral (Fig. 8c) [18]. The exothermic effect is insignificant and its peak falls at the temperature of 870°C, which confirms the disorder in the structure of kaolinite [19].

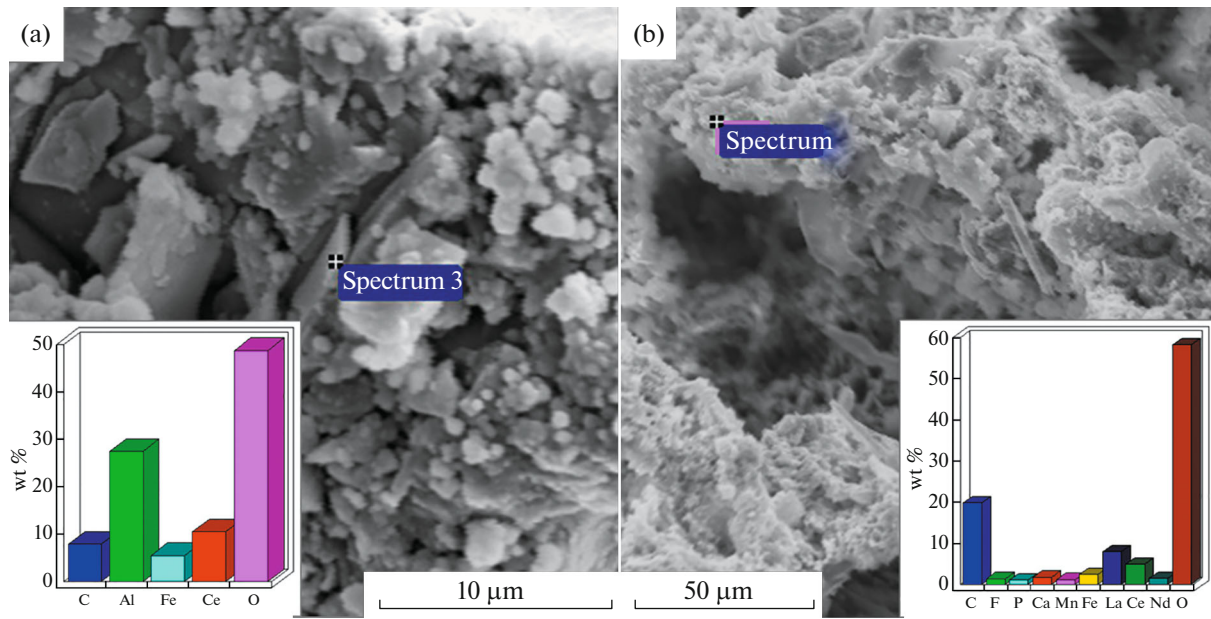


Fig. 4. Biofilms: (a) gibbsite, (b) on the wall of the cavity in LKV. Inset EMF composition. SAM.

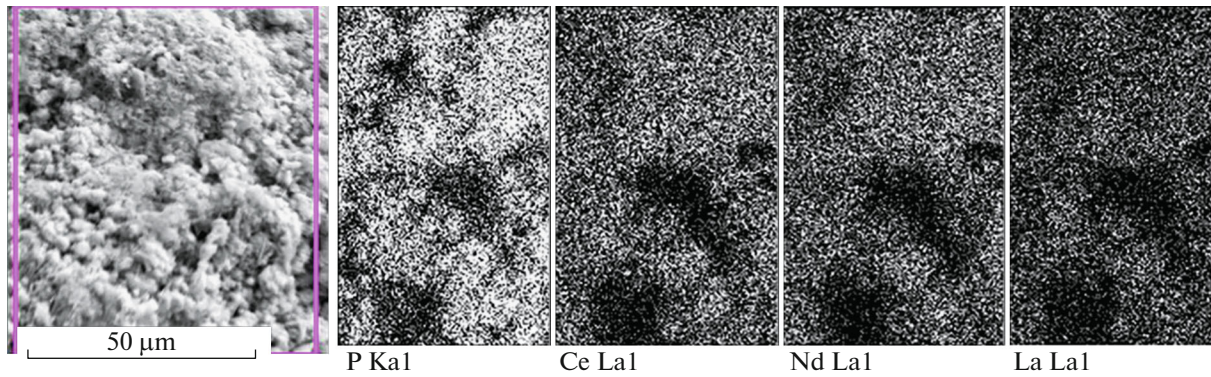


Fig. 5. Microcrystalline substance, REE distribution. EDS composition. SEM.

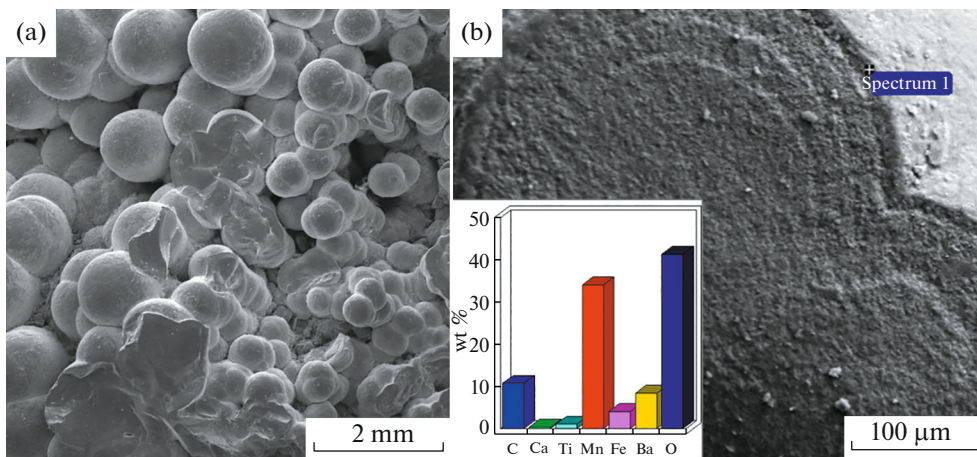


Fig. 6. Psilomelane. Inset: EDS composition. SEM.

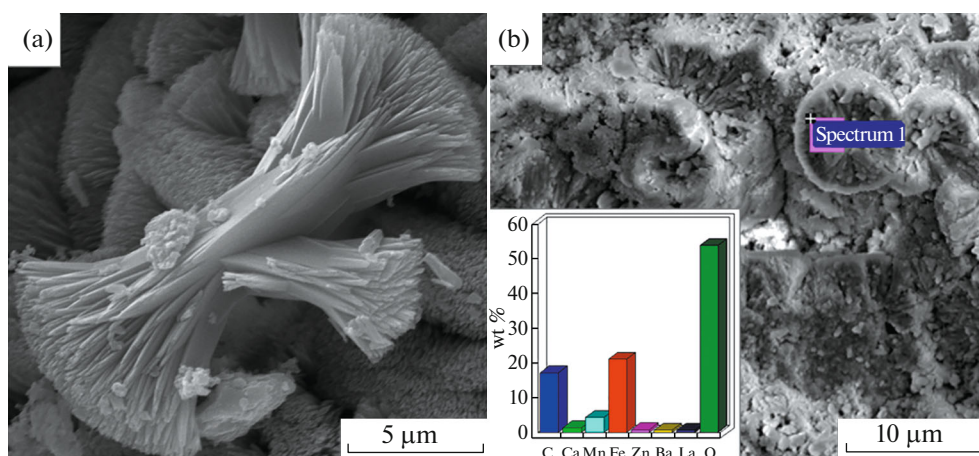


Fig. 7. Goethite in bauxite. Inset: EDS composition. SEM.

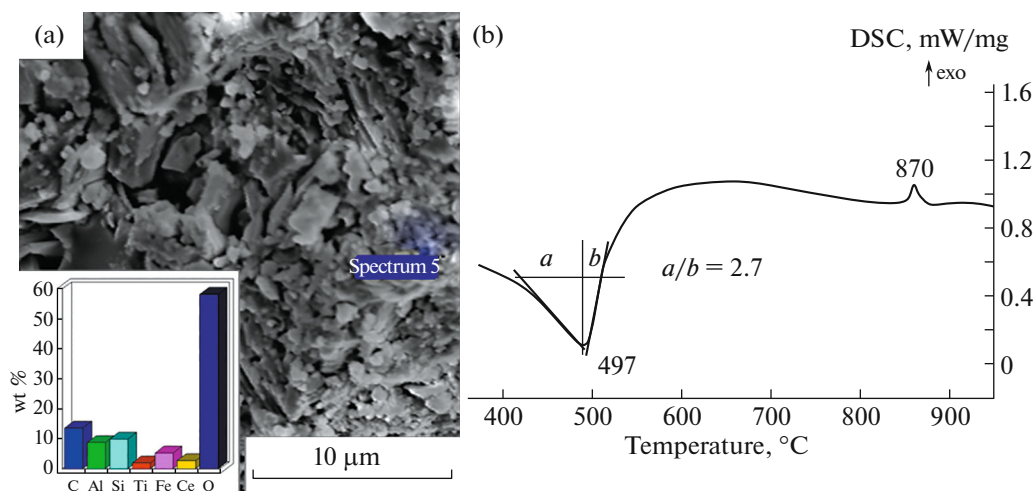


Fig. 8. (a) Kaolinite and its EDS composition, (b) SEM, DSC curve of kaolinite.

CONCLUSIONS

The bauxite deposits of the Russian Federation are few and are characterized by a relatively low content of useful components due to the climate conditions of formation. Deposits of bauxites of the Chadobets group are accepted on the state balance only as aluminum raw materials with the associated extraction of gallium and vanadium [20]. The high concentrations of rare metals and REE found in the bauxites of the Tsentral'noe deposit allow us to consider them as a complex mineral raw material. The study of the geological structure of the deposit, of the morphology of ore-forming bauxite minerals, and of their composition has made it possible to substantiate their genesis and determine the sources of ore matter. Bauxites are the total product of lateritic weathering of all rocks composing the northern dome of the Chadobets uplift and their partial denudation and accumulation in erosional depressions. The forms of rare metals and REE

minerals identified characterize their supergene nature. Their fragility and dispersion complicate the mechanical extraction of useful components and make one prefer hydrometallurgical methods of ore processing. The source rare-earth and trace elements is carbonatites, with which the niobium–rare metal Chuktukon deposit is associated. The laterization of these rocks together with quartz–muscovite–feldspar schists and subsequent denudation led to the formation of unique bauxite deposits with a high content of REEs, Ti, Sr, Ba, P, U, and Th.

FUNDING

This work was supported by the Ministry of Education and Science of Russia, grant no. 075-15-2020-802, and analytical studies were carried out at the IGEM ANALITIKA Center for Collective Use.

REFERENCES

1. A. V. Lapin and A. V. Tolstov, *Deposits of Carbonatite Weathering Crusts* (Nauka, Moscow, 1995) [in Russian].
2. A. V. Lapin, I. M. Kulikova, and E. N. Levchenko, in *Rare Metal Deposits: New Data on Mineralogy and Geochemistry* (Inst. Mineral., Geochem. Crystal Chem. Rare Elements, Moscow, 2017), pp. 102–114 [in Russian].
3. V. I. Kuz'min, D. V. Kuz'min, and A. M. Zhizhaev, *J. Sib. Federal Univ. Chem.*, No. 3, 303–312 (2013).
4. A. D. Slukin, *Winding Cores and Bauxites of Chadobetskii Plateau* (Nauka, Moscow, 1973) [in Russian].
5. D. A. Monsels, Thesis (Utrecht, 2018).
6. X. Wang, Y. Jiao, Y. Du, et al., *J. Geochem. Explor.* **133**, 103–117 (2013).
7. J. J. Braun, M. Page, A. Herbillin, and C. Rosin, *Geochim. Cosmochim. Acta* **57** (18), 4419–4434 (1993). [https://doi.org/10.1016/0016-7037\(93\)90492-F](https://doi.org/10.1016/0016-7037(93)90492-F)
8. L. E. Mordberg, C. J. Stanley, and K. Germann, *Mineral. Mag.* **65** (1), 81–101 (2001).
9. V. I. Sirotnin, V. A. Shatrov, G. V. Voitsekhovskii, et al., *Lithol. Miner. Resour.* **40** (3), 216–232 (2005).
10. V. L. Onana, R. F. D. Ntoulala, and S. N. Tangc, *J. Afr. Earth Sci.* **124**, 371–382 (2016).
11. A. D. Slukin, N. S. Bortnikov, V. M. Novikov, N. M. Boeva, A. P. Zhukhlistov, E. A. Zhegallo, and L. V. Zaitseva, in *Proc. All-Russ. Conf. Depositions of Strategic Metals: Location Regularities, Matter Sources, Formation Conditions and Mechanisms* (Inst. Geol. Ore Deposits, Petrogr., Mineral., Geochem. Russ. Acad. Sci., Moscow, 2015), pp. 241–242 [in Russian].
12. V. I. Mamedov, A. A. Chausov, E. A. Okonov, M. A. Makarova, and N. M. Boeva, *Geol. Ore Deposits* **56** (2), 163–176 (2020). <https://doi.org/10.1134/S1075701520020026>
13. V. I. Mamedov, M. A. Makarova, N. M. Boeva, A. D. Slukin, E. S. Shipilova, N. S. Bortnikov, *Dokl. Earth Sci.* **492** (1), 291–296 (2020). <https://doi.org/10.1134/S1028334X20050128>
14. A. D. Slukin, N. S. Bortnikov, L. V. Zaytseva, A. P. Zhukhlistov, A. V. Mokhov, and N. M. Boeva, in *Biogenic-Abiogenic Interactions in Natural and Anthropogenic Systems*, Ed. by O. V. Frank-Kamenetskaya, E. G. Panova, and D. Yu. Vlasov (Springer, 2015), pp. 67–75.
15. V. M. Novikov, N. M. Boeva, N. S. Bortnikov, A. P. Zhukhlistov, V. V. Krupskaya, and E. B. Bushueva, *Geol. Ore Deposits* **60** (6), 513–526 (2018). <https://doi.org/10.1134/S107570151806003X>
16. N. S. Bortnikov, V. M. Novikov, A. D. Savko, N. M. Boeva, E. A. Zhegallo, E. B. Bushueva, A. V. Kraïnov, and D. A. Dmitriev, *Lithol. Miner. Resour.* **48** (5), 384–397 (2013).
17. N. L. Dobretsov, S. M. Zhmodik, E. V. Lazareva, A. V. Bryanskaya, V. A. Ponomarchuk, B. Yu. Sarygool, I. S. Kirichenko, A. V. Tolstov, and N. S. Karmanov, *Dokl. Earth Sci.* **496** (2), 135–139 (2021).
18. E. V. Lazareva, S. M. Zhmodik, N. L. Dobretsov, A. V. Tolstov, B. L. Shcherbov, N. S. Karmanov, E. Yu. Gerasimov, and A. V. Bryanskaya, *Geol. Geofiz.* **56** (6), 1080–1115 (2015).
19. V. M. Sinitsyn, *Climate of Laterite and Bauxite* (Nedra, Leningrad, 1976) [in Russian].
20. B. V. Shibistov, *Zh. Sib. Fed. Univ. Tekhn. Tekhnol.* **8** (6), 995–1002 (2013).

Translated by M.S. Nickolsky